

Supplementary information for

Surface available gravitational potential energy in the world oceans

Ruixin Huang², Bo Qiu³, Zhiyou Jing^{1*}

¹State Key Laboratory of Tropical Oceanography, South China Sea Institute of Oceanology, Chinese Academy of Sciences, Guangzhou 510301, China

²Woods Hole Oceanographic Institution, Woods Hole, MA 02543, USA

³Department of Oceanography, University of Hawaii at Manoa, Honolulu, Hawaii 96822, USA

Contents of this file

Discussion on the classical Rossby adjustment problem and Figs S1 to S4

Supplementary Figs of ASPE and surface KE based on a 7.5 km-resolution ROMS simulation data. S5

S.1 The Rossby adjustment of a homogeneous fluid

Consider a homogeneous ocean of constant depth H . At time $t=0$, there is a uniform current jet (width of $2b$) of speed U_0 into the page. The initial solution is denoted in upper case characters, (Y, U) ; the solution after adjustment in the new coordinates is denoted in lower case characters, (y, u) . The x-momentum equation and its time integration lead to

$$du/dt = fv, \quad u - U = f(y - Y). \quad (S1)$$

The continuity condition is,

$$h = HdY/dy. \quad (S2)$$

The final state is in geostrophy

$$u = -\frac{g}{f} \frac{dh}{dy}. \quad (S3)$$

A single equation for Y is

$$\frac{d^2Y}{dy^2} - \frac{Y}{\lambda^2} = -\frac{y}{\lambda^2} - \frac{U}{f\lambda^2}, \quad (S4)$$

where $\lambda = \sqrt{gH}/f$ is the Rossby radius of deformation. The solution is found by matching three pieces of solution over two locations as shown in Fig. S1.

The total kinetic energy and surface potential energy in the initial state are

$$K_0 = b\rho_0HU_0^2, \quad \chi_0 = 0. \quad (S5)$$

In the final state the total kinetic energy in these three regions are

$$K_{II,1} = \frac{\rho_0\lambda HU_0^2 e^{-2b/\lambda}}{8} (e^{2b/\lambda} - e^{-2b/\lambda} + 4b/\lambda), \quad (S6)$$

$$K_{I,1} = K_{III,1} = \frac{\rho_0 \lambda H U_0^2}{4} \sinh^2(b/\lambda) e^{-2b/\lambda}, \quad (S7)$$

$$K_1 = K_{I,1} + K_{II,1} + K_{III,1} = \frac{\rho_0 \lambda H U_0^2}{8} e^{-2b/\lambda} \left(2e^{2b/\lambda} - 2 + \frac{4b}{\lambda} \right). \quad (S8)$$

The total surface potential energy in these three regions is

$$\chi_{II,1} = \frac{\rho_0 \lambda H U_0^2}{8} e^{-2b/\lambda} \left(e^{2b/\lambda} - e^{-2b/\lambda} - 4b/\lambda \right), \quad (S9)$$

$$\chi_{I,1} = \chi_{III,1} = \frac{\rho_0 \lambda H U_0^2}{4} \sinh^2(b/\lambda) e^{-2b/\lambda}. \quad (S10)$$

Thus, the total kinetic energy in region I and III is

$$K_{I,1} + K_{III,1} = \chi_{I,1} + \chi_{III,1} = \frac{\rho_0 \lambda H U_0^2}{2} e^{-2b/\lambda} \sinh^2(b/\lambda). \quad (S11)$$

Accordingly, energy in the final state is equally participant between the kinetic energy and the surface potential energy.

The total surface potential in the final state is

$$\chi_1 = \chi_{I,1} + \chi_{II,1} + \chi_{III,1} = \frac{\rho_0 \lambda H U_0^2}{8} e^{-2b/\lambda} \left(2e^{2b/\lambda} - 2 - \frac{4b}{\lambda} \right). \quad (S12)$$

The total energy after adjustment is

$$K_1 + \chi_1 = \frac{\rho_0 \lambda H U_0^2}{2} (1 - e^{-2b/\lambda}). \quad (S13)$$

When $b/\lambda \ll 1$, the asymptotic solution is

$$u'' = U_0 \left[1 - \frac{b}{\lambda} + \frac{b^2}{2\lambda^2} \left(1 + \frac{y^2}{b^2} \right) \right] + o\left(\frac{b}{\lambda}\right)^2 \approx U_0 \quad (S14)$$

Thus, the velocity field is basically unchanged.

$$K_{II,1} \approx \rho_0 b H U_0^2 \left(1 - \frac{2b}{\lambda} + \frac{3b^2}{\lambda^2} \right) < K_0, \quad (S15)$$

$$\chi_{II} \approx \frac{\rho_0 b H U_0^2}{3} \left(1 - \frac{2b}{\lambda} \right) \frac{b^2}{\lambda^2} \ll K_0, \quad (S16)$$

$$K_{I,1} + K_{III,1} = \chi_{I,1} + \chi_{III,1} \approx \frac{\rho_0 b H U_0^2}{2} \left(1 - \frac{2b}{\lambda} \right) \frac{b}{\lambda} \ll K_0, \quad (S17)$$

$$K_1 + \chi_1 = \frac{\rho_0 \lambda H U_0^2}{2} (1 - e^{-2b/\lambda}) \approx \rho_0 b H U_0^2 \left(1 - \frac{b}{\lambda} \right) = K_0 \left(1 - \frac{b}{\lambda} \right). \quad (S18)$$

Hence, in the final state the energy is mostly retained in region II and in the form of kinetic energy associated with the geostrophically balanced velocity, while the potential energy associated with the pressure field consists of a very small portion. The energy dispersed to the originally rest part of the ocean is quite small.

If $b/\lambda \gg 1$, the approximate solution is in the following forms

$$u(0) = U_0 e^{-b/\lambda} \approx 0; \quad (S19a)$$

$$u(-b^-) = u(b^+) = -U_0/2; \quad (S19b)$$

$$u(b^-) = u(-b^+) = U_0/2. \quad (S19c)$$

Away from these two pivotal points, the final velocity is practically zero. Thus, if the initial velocity jet is much wider than the deformation radius, the velocity field is totally destroyed.

The total energy in this case is

$$K_1 + \chi_1 = \frac{\rho_0 \lambda H U_0^2}{2} (1 - e^{-2b/\lambda}) \approx \frac{\rho_0 \lambda H U_0^2}{2} \ll K_0. \quad (S20)$$

Thus, most of the energy originally stored in the form of kinetic energy is dissipated during the process of geostrophic adjustment. According to the classical theory of geostrophic adjustment, the gravity waves play a vitally important role. For a model ocean sitting on an infinite f-plane, most of the original energy is lost to the infinity through gravity wave radiation during the adjustment.

S.2 The adjustment with an initial finite step in free surface

The second case is with an initially single step-like perturbation in sea surface for an ocean at rest, Fig. S2. The solution in these two regions are

$$Y_I = y + Be^{y/\lambda_I}, \quad Y_{II} = y + Ae^{-y/\lambda_{II}}, \quad (S21)$$

where $\lambda_I = \sqrt{g(H + \Delta H)} / f$ and $\lambda_{II} = \sqrt{gH} / f$ are the deformation radius for domain I and II.

The total kinetic energy in these two regions is

$$K_{I,1} \approx \frac{\rho_0 H f^2 \lambda_{II}^3 \Delta^2}{16}, \quad K_{II,1} \approx \frac{\rho_0 H f^2 \lambda_{II}^3 \Delta^2}{16}, \quad (S22)$$

$$\chi_{II,1} \approx -\frac{3\rho_0 H f^2 \lambda_{II}^3 \Delta^2}{32}, \quad \chi_{I,1} \approx -\frac{3\rho_0 H f^2 \lambda_{II}^3 \Delta^2}{32}. \quad (S23)$$

Thus, the total loss in potential energy is

$$\chi_{I,1} + \chi_{II,1} \approx -\frac{3\rho_0 H f^2 \lambda_{II}^3 \Delta^2}{16}. \quad (S24)$$

The total gain in kinetic energy is

$$K_{I,1} + K_{II,1} \approx \frac{2\rho_0 H f^2 \lambda_{II}^3 \Delta^2}{16}. \quad (S25)$$

Since the initial state has a scale much larger than the radius of deformation, the pressure field is mostly retained, except near the front, and most energy associated with the initial pressure perturbation is retained. After the adjustment, the geostrophic velocity field is established. There is about 1/3 of the surface potential energy is dispersed to infinite through gravity wave radiation during the adjustment.

S.3 The adjustment with an initial finite step of finite width in free surface

The case with an initial step-like perturbation of free surface elevation is of great interest. The model domain can be separated into three sub-regions, as shown in Fig. S3.

The solutions in these domains are

$$Y_I = y + Ae^{y/\lambda_I}, \quad Y_{II} = y + Be^{y/\lambda_{II}} + Ce^{-y/\lambda_{II}}, \quad Y_{III} = y + De^{-y/\lambda_I}, \quad (S26)$$

where $\lambda_I = \sqrt{gH} / f$ and $\lambda_{II} = \sqrt{g(H + \Delta H)} / f$ are the deformation radius for domain I and II.

The layer thickness is

$$h_I = H dY_I / dy, h_{II} = H(1 + \Delta) dY_{II} / dy, h_{III} = H dY_{III} / dy, \quad (S27)$$

where $\Delta = \Delta H / H \ll 1$ in general. The constants A, B, C and D are determined by matching boundary conditions.

In domain II, potential energy before and after adjustment is

$$\chi_{II,0} = \rho_0 g b H^2 (1 + 2\Delta + \Delta^2), \quad (S28)$$

$$\chi_{II,1} = \rho_0 g b (H + \Delta H)^2 \left\{ 1 + \frac{B^2}{\lambda_{II} b} \frac{2b}{\lambda_{II}} \left(1 + \frac{4b^2}{6\lambda_{II}^2} \right) + \frac{4B}{\lambda_{II}} \left(1 + \frac{b^2}{\lambda_{II}^2} \right) + 2 \frac{B^2}{\lambda_{II}^2} \right\}. \quad (S29)$$

For domain I

$$\chi_{I,1} - \chi_{I,0} = \frac{\rho_0 g H^2}{2} \left(\frac{A^2}{2\lambda_I} e^{-2b/\lambda_I} + 2Ae^{-b/\lambda_I} \right), \quad (\text{S30})$$

When $b \ll \lambda_I, \lambda_{II}$,

$$\chi_{II,0} - \chi_{II,1} \approx 2\rho_0 f^2 H \Delta b \lambda_I^2. \quad (\text{S31})$$

The total potential energy change in region I and III is

$$(\chi_{I,1} + \chi_{III,1}) - (\chi_{I,0} + \chi_{III,0}) = 2(\chi_{I,1} - \chi_{I,0}) \approx 2\rho_0 f^2 H \Delta b \lambda_I^2. \quad (\text{S32})$$

Equations (S31) and (S32) show that the potential energy loss in region II is mostly converted into potential energy gain in region I and III. This potential energy transport between region II and regions I/III indicates that there is little energy conversion from the potential energy into kinetic energy for the limit of $b \ll \lambda_{II}$.

The kinetic energy for domain I is

$$K_{I,1} = \frac{\rho_0 f^2 H \Delta^2 b^2}{2} \left(\frac{\lambda_I}{2} e^{-b/\lambda_I} + \frac{A}{3} e^{-2b/\lambda_I} \right). \quad (\text{S33})$$

For domain II, it is

$$K_{II,1} = -\frac{\rho_0 f^2 H (1 + \Delta)^2 B^2}{2} \left[\frac{8b^3}{3\lambda_{II}^2} + \frac{20b}{3\lambda_{II}} B \right], \quad (\text{S34})$$

When $b \ll \lambda_I, \lambda_{II}$,

$$K_{I,1} \approx 2\rho_0 f^2 H \Delta b \lambda_I^2 * \frac{\Delta b}{8\lambda_I} \ll (\chi_{II,0} - \chi_{II,1}), \quad (\text{S35})$$

$$K_I + K_{III} = 2K_{I,1} \ll (\chi_{I,0} - \chi_{I,1}), \quad (\text{S36})$$

$$K_{II,1} \approx \frac{5}{6} \rho_0 f^2 H \Delta^3 b \lambda_{II} \quad , \quad (S37)$$

Since $\chi_{II,0} - \chi_{II,1} \approx 2\rho_0 f^2 H \Delta b \lambda_I^2$, kinetic energy gain in region II is much smaller than that converted to the kinetic energy in this region.

When the width of the initial step in free surface is much larger than the deformation radius, change in the free surface elevation is mostly confined to the vicinity of the initial front with the order of deformation radius.

S.4 On the relation between APE and ASPE in a $2\frac{1}{2}$ layer ocean

Assuming hydrostatic approximation and the second layer is very thick and motionless, there is a simple relation

$$\rho_0 \nabla \eta = \Delta \rho \nabla h_1 \quad . \quad (S38)$$

As shown in Fig. S4b, in the physical state, there is a light water upper layer and a slightly dense lower layer occupying the water column. The mean thickness of these two layers are h_{10} and h_{20} . The interface between the upper and lower layers is slanted, and the depth change over the width of the water column is $2H$. Assuming the second layer is stagnant, thus the free surface elevation has a slope opposite of that of the interface, and the corresponding change of sea level across the width of the water column is $2N$.

According to Eq. (S38), there is a simple relation between N and H

$$\rho_0 N = \Delta \rho H \quad . \quad (S39)$$

The thickness of the first and second layer is

$$h_1 = h_{10} + \frac{2(H+N)}{b} \left(x - \frac{b}{2} \right), \quad h_2 = h_{20} - \frac{2H}{b} \left(x - \frac{b}{2} \right). \quad (\text{S40})$$

The total amount of gravitational potential energy of layer 2 is

$$\chi_2 = g \frac{\rho_0 + \Delta\rho}{2} h_{20}^2 b + g \frac{\rho_0 + \Delta\rho}{6} H^2 b \quad (\text{S41})$$

Thus, the total gravitational potential energy of the upper layer is

$$\chi_1 = g\rho_0 \int_0^b \left[h_{20} - \frac{2H}{b} \left(x - \frac{b}{2} \right) + \frac{h_1}{2} \right] h_1 dx \quad (\text{S42})$$

After manipulating, this leads to

$$\chi_1 = g\rho_0 \left(h_{20} + \frac{h_{10}}{2} \right) h_{10} b - g\rho_0 \frac{H^2 - N^2}{6} b, \quad (\text{S43})$$

$$(\chi_1 + \chi_2) - (\chi_{1,0} + \chi_{2,0}) = \frac{g\Delta\rho H^2 b}{6} + \frac{g\rho_0 N^2 b}{6}, \quad (\text{S44})$$

where,

$$\chi_{bc} = \frac{g\Delta\rho H^2 b}{6}, \quad \chi_s = \frac{g\rho_0 N^2 b}{6} \quad (\text{S45})$$

are the baroclinic APE and the ASPE. In general, $\Delta\rho / \rho_0 \approx 0.001 - 0.003$; thus, ASPE is much smaller than APE.

The corresponding geostrophic velocity is $u = g'2H / fb$; thus, the total kinetic energy for the upper layer is

$$K = 0.5\rho_0 h_{10} b u^2 = 2g\Delta\rho H h_{10} b \left(\frac{\lambda}{b} \right)^2 \quad (\text{S46})$$

The ratio of APE vs KE is

$$\chi_{bc} / K = 12 \left(\frac{h_{10}}{H} \right) \left(\frac{\lambda}{b} \right)^2. \quad (\text{S47})$$

If the width of the original jet is much larger than the deformation radius, the APE is much larger than kinetic energy.

Figures

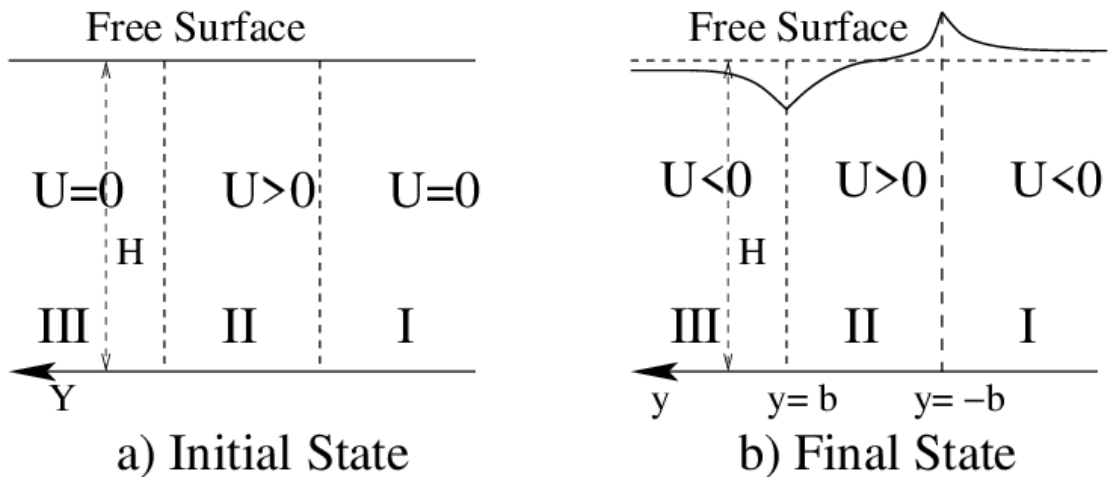


Fig. S1. The Rossby problem for a homogeneous ocean with an initial velocity jet (looking toward the east).

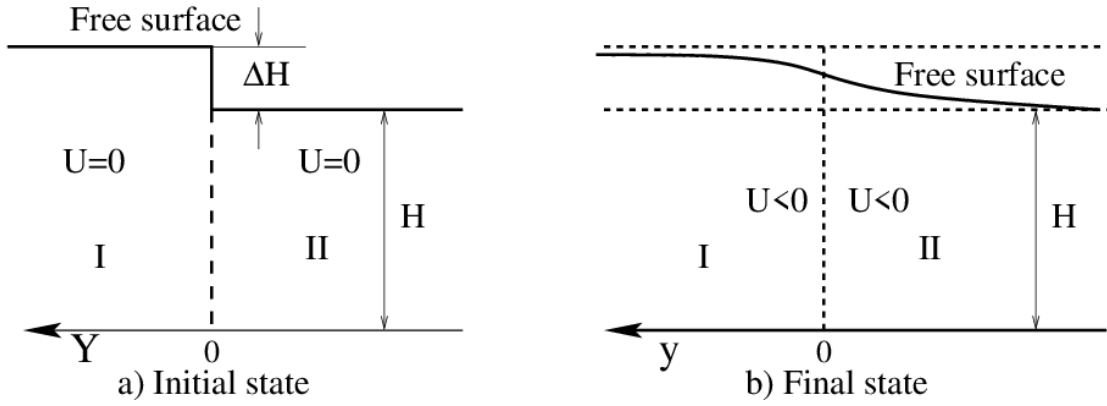


Fig. S2. Geostrophic adjustment induced by an initial step in sea surface elevation.

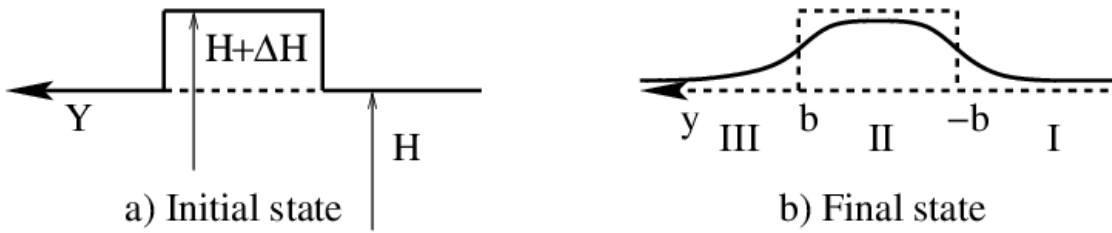


Fig. S3. Adjustment of an initial step of finite width of free surface elevation.

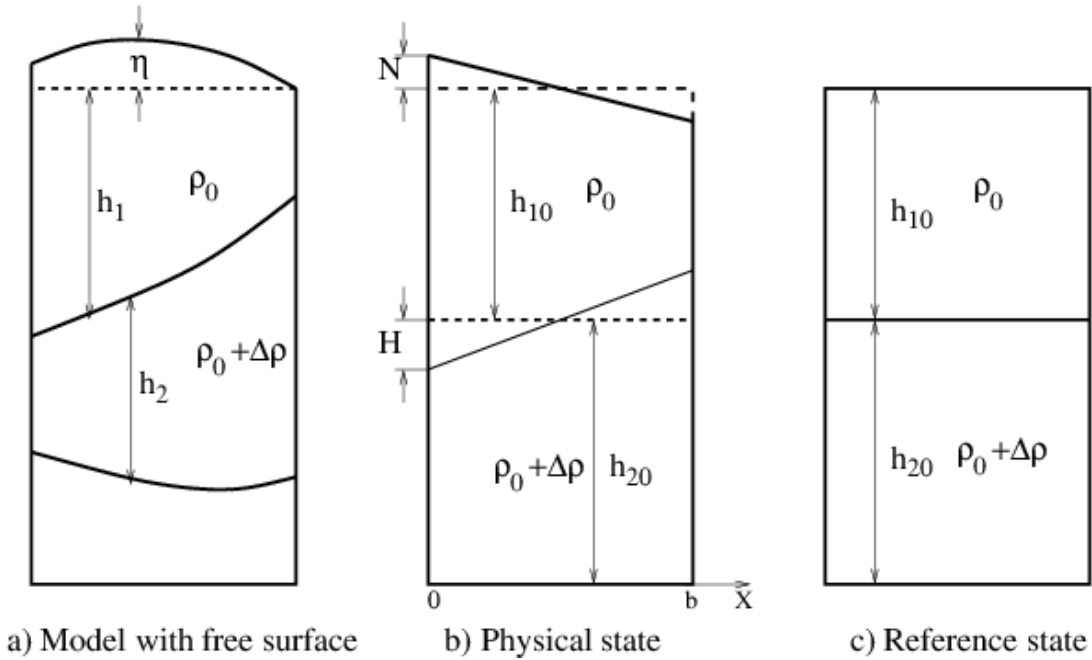


Fig. S4. Sketch of the model ocean.

S.5 Supplementary Figs of ASPE and surface KE based on a 7.5 km-resolution ROMS simulation data

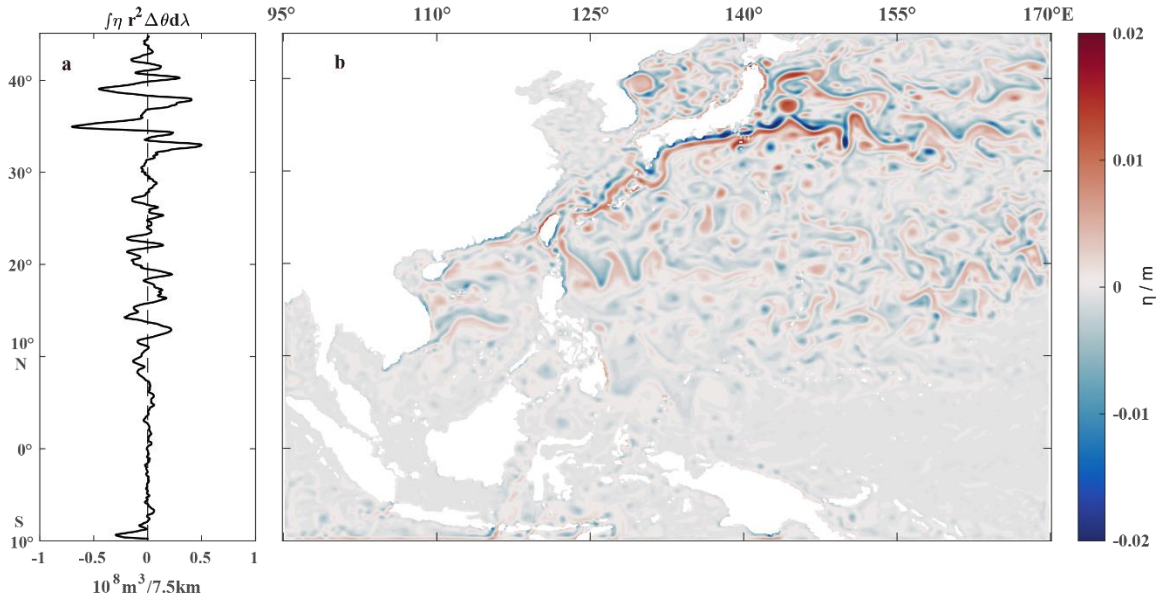


Fig. S5. The Northwest Pacific SSH in the scale of <20 km (roughly following a 3-point scheme), July 15, 2003, based on the converted ROMS data.

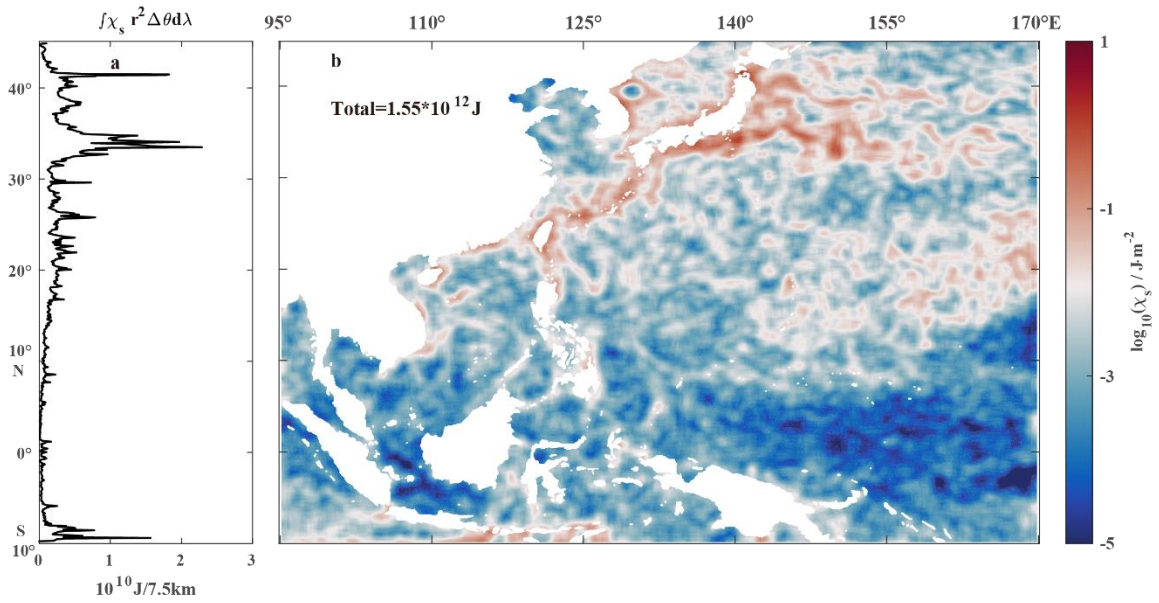


Fig. S6. The Northwest Pacific ASPE in the scale of <20 km, July 15, 2003, based on the converted ROMS data.

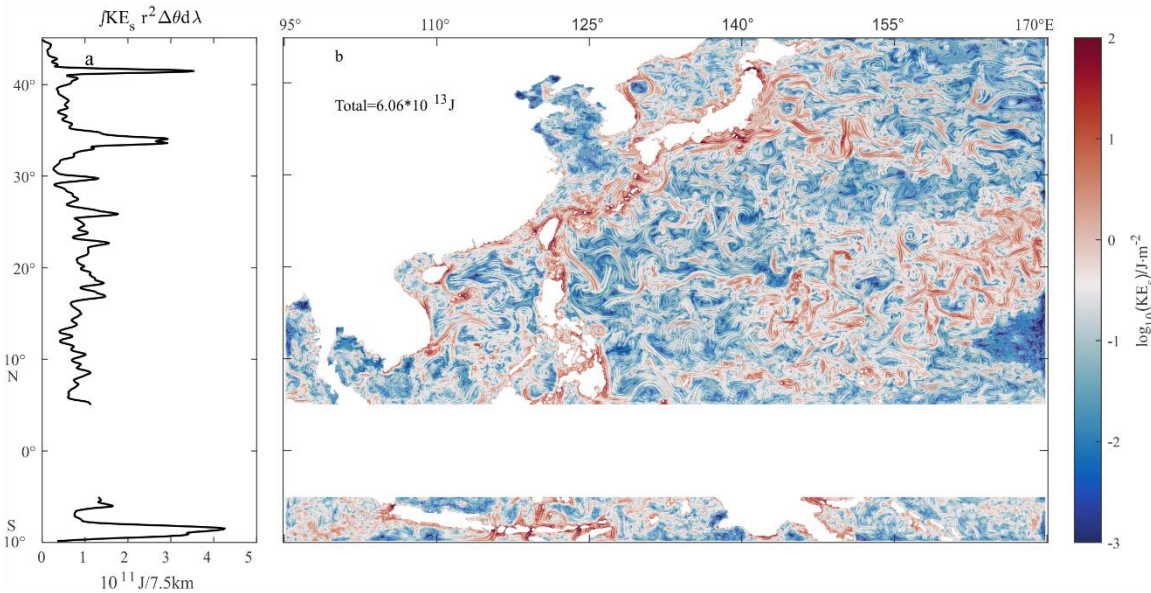


Fig. S7. The Northwest Pacific surface KE in the scale of <20 km, July 15, 2003, based on the converted ROMS data.

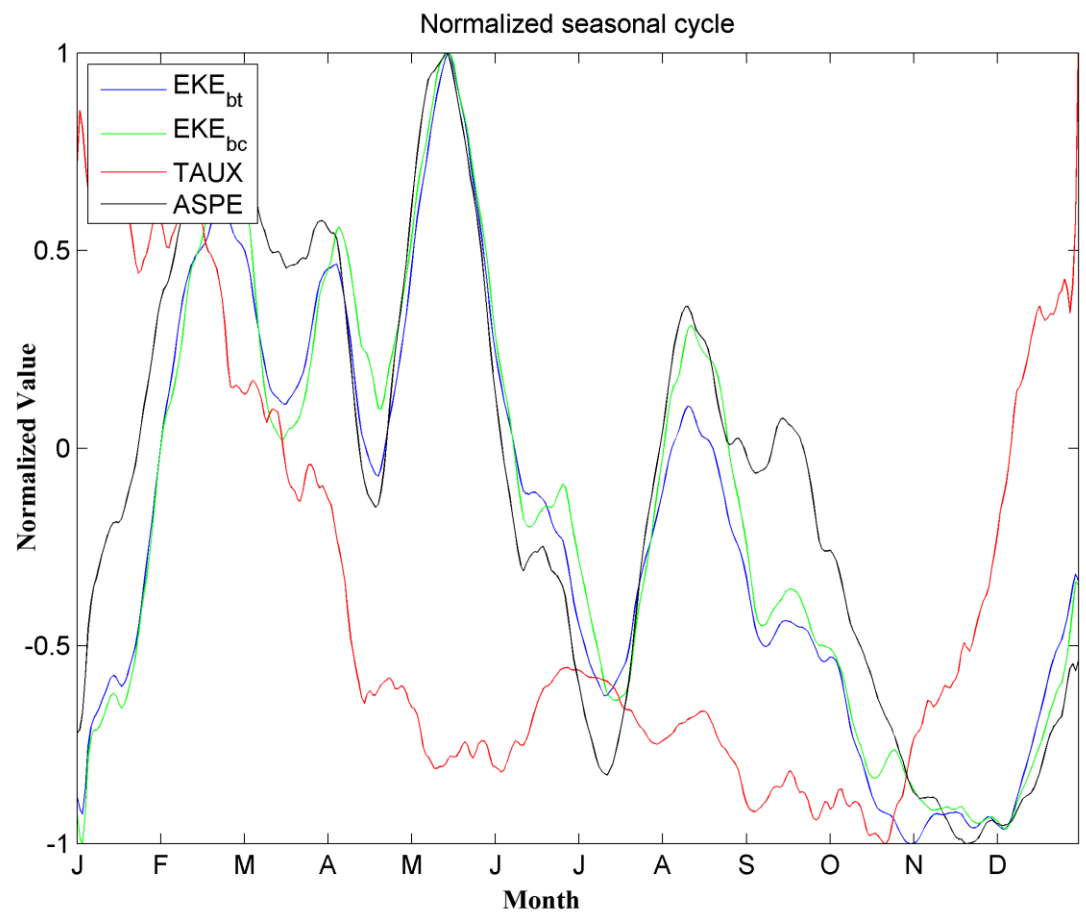


Fig. S8. Normalized seasonal cycle of ASPE, EKE_{BT} , EKE_{BC} and zonal wind stress in the scale of <20 km over the Kuroshio extension region, based on the converted ROMS data. The correlation coefficients between the ASPE and two EKE components (EKE_{BT} , EKE_{BC}) are 0.94 and 0.92, separately.

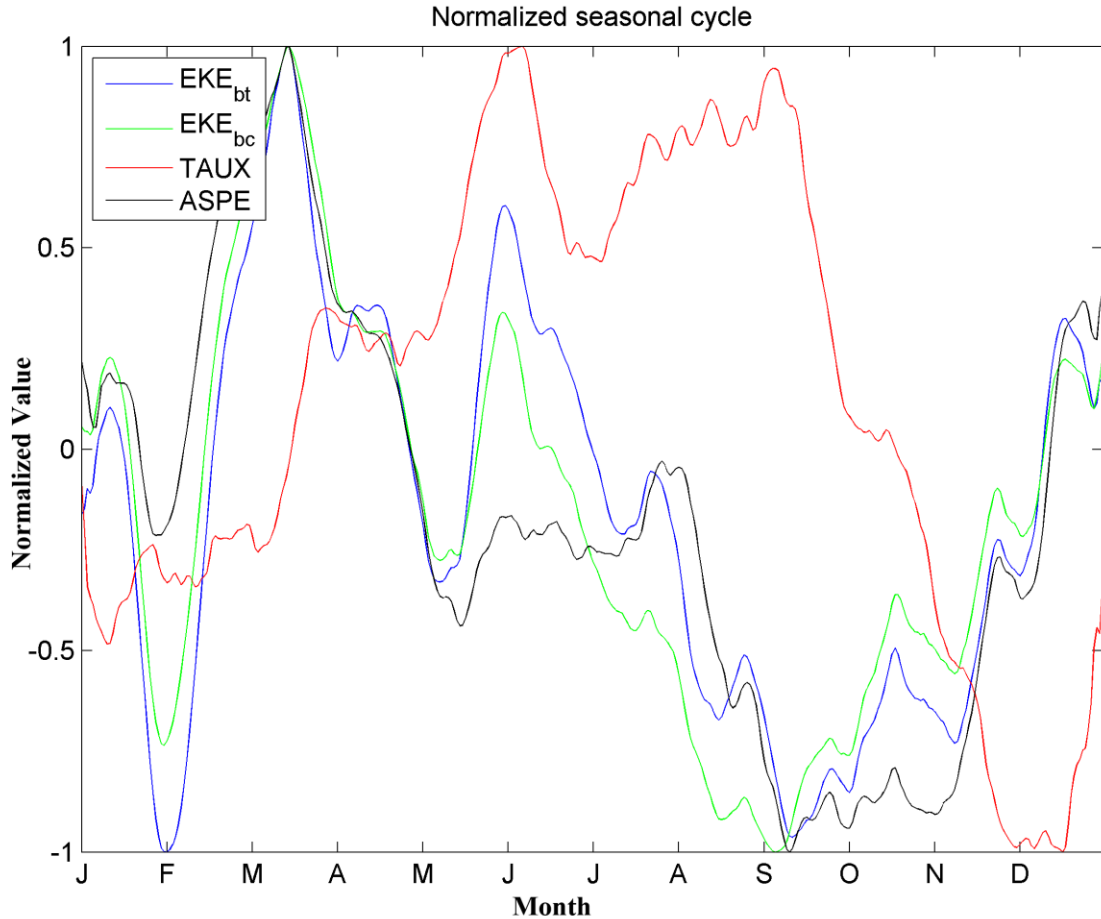


Fig. S9. Normalized seasonal cycle of ASPE, EKE_{BT} , EKE_{BC} and zonal wind stress in the scale of <20 km over the STCC region, based on the converted ROMS data. The correlation coefficients between the ASPE and two EKE components (EKE_{BT} , EKE_{BC}) are 0.81 and 0.86, separately.

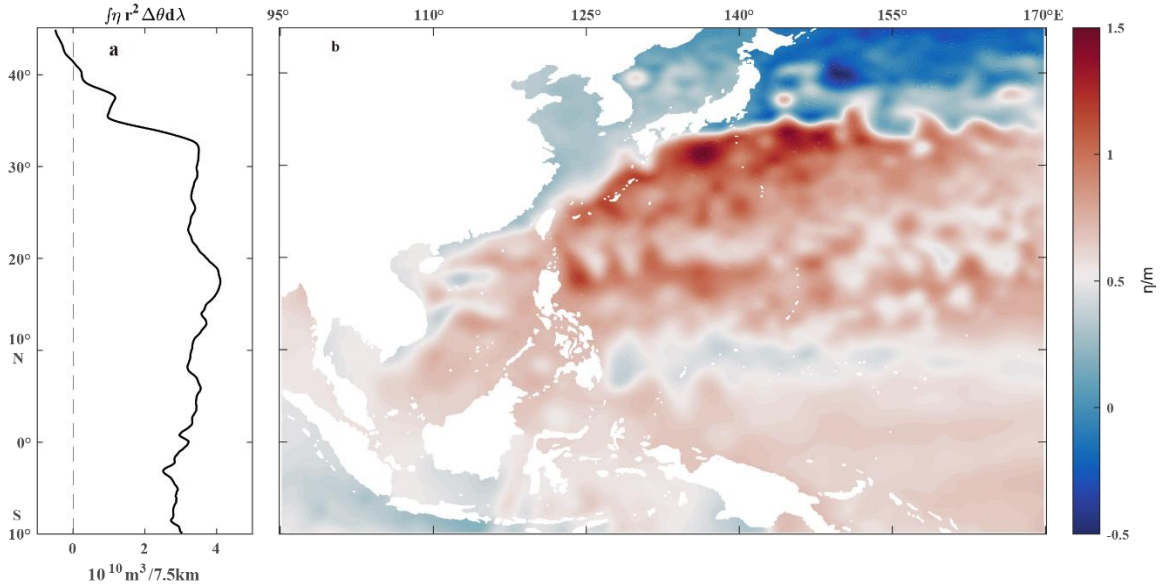


Fig. S10. The Northwest Pacific SSH in the scale of >50 km (roughly following a 7-point scheme), July 15, 2003, based on the converted ROMS data.

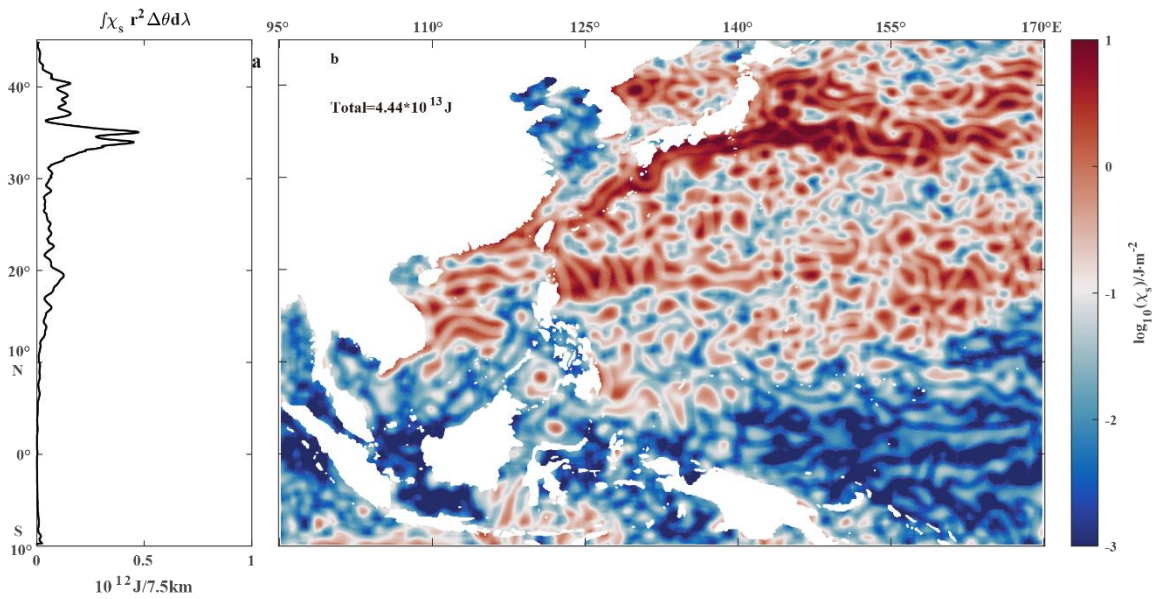


Fig. S11. The Northwest Pacific ASPE in the scale of >50 km, July 15, 2003, based on the converted ROMS data.

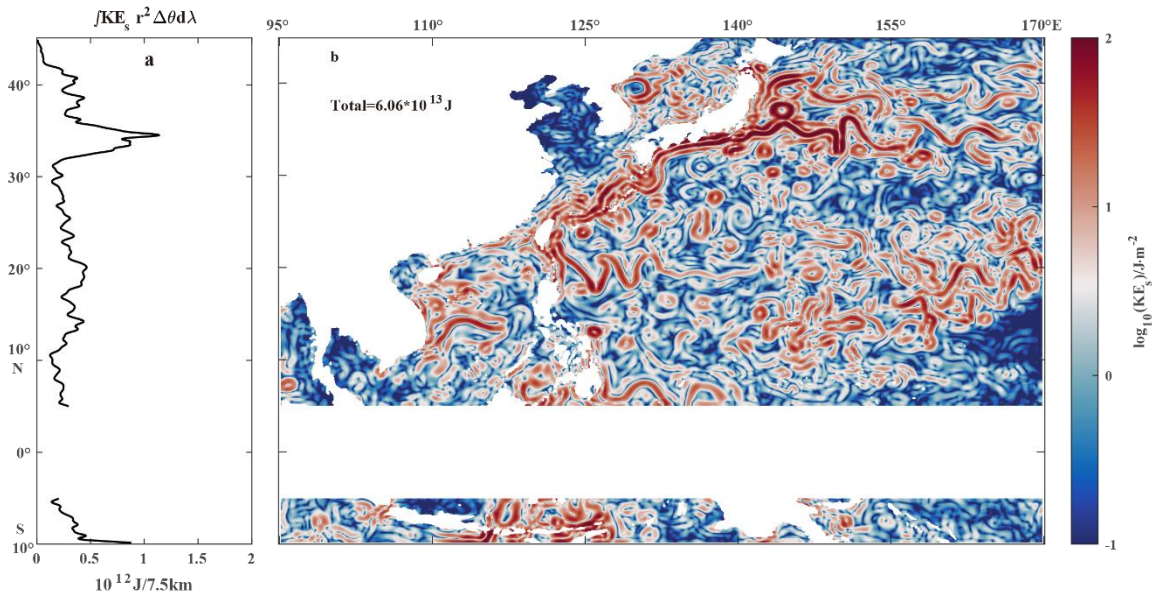


Fig. S12. The Northwest Pacific surface KE in the scale of >50 km, July 15, 2003, based on the converted ROMS data.

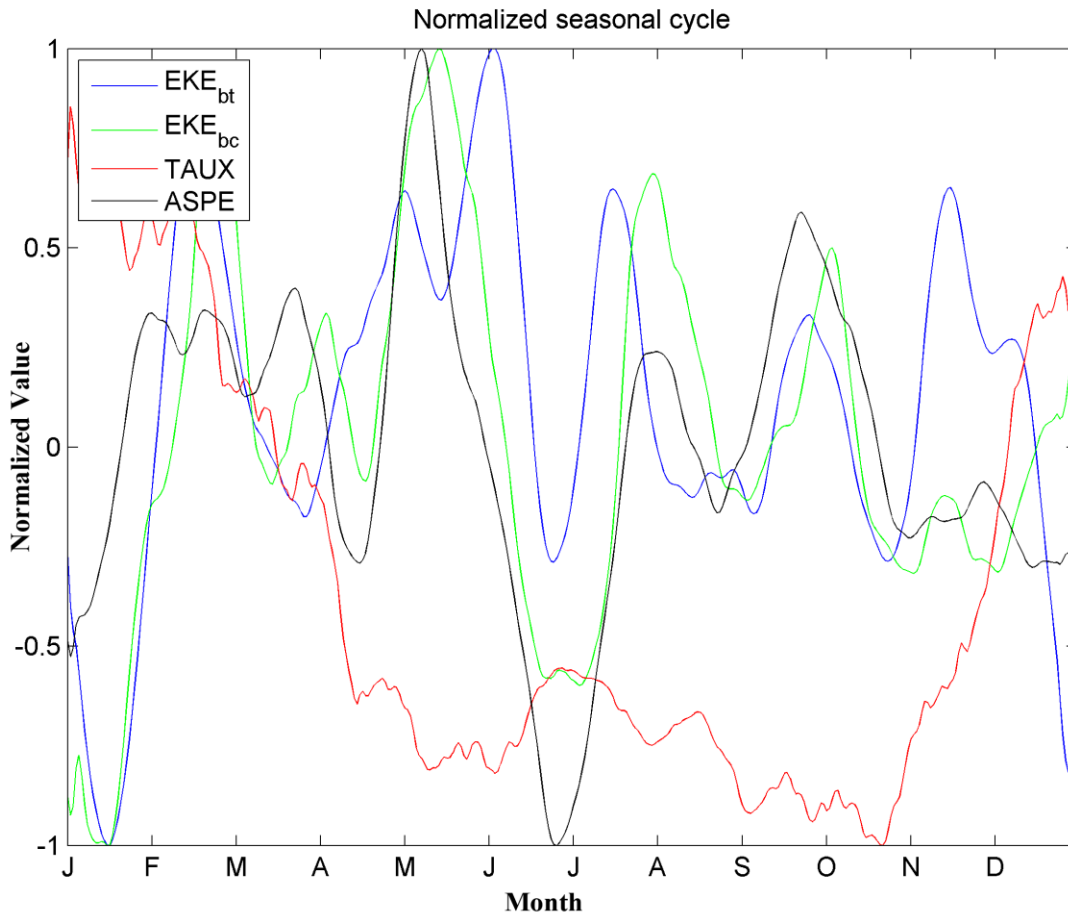


Fig. S13. Normalized seasonal cycle of ASPE, EKE_{BT} , EKE_{BC} and zonal wind stress in the scale of >50 km over the Kuroshio extension region, based on the converted ROMS data. The correlation coefficients between the ASPE and two EKE components (EKE_{BT} , EKE_{BC}) are 0.28 and 0.71, separately.

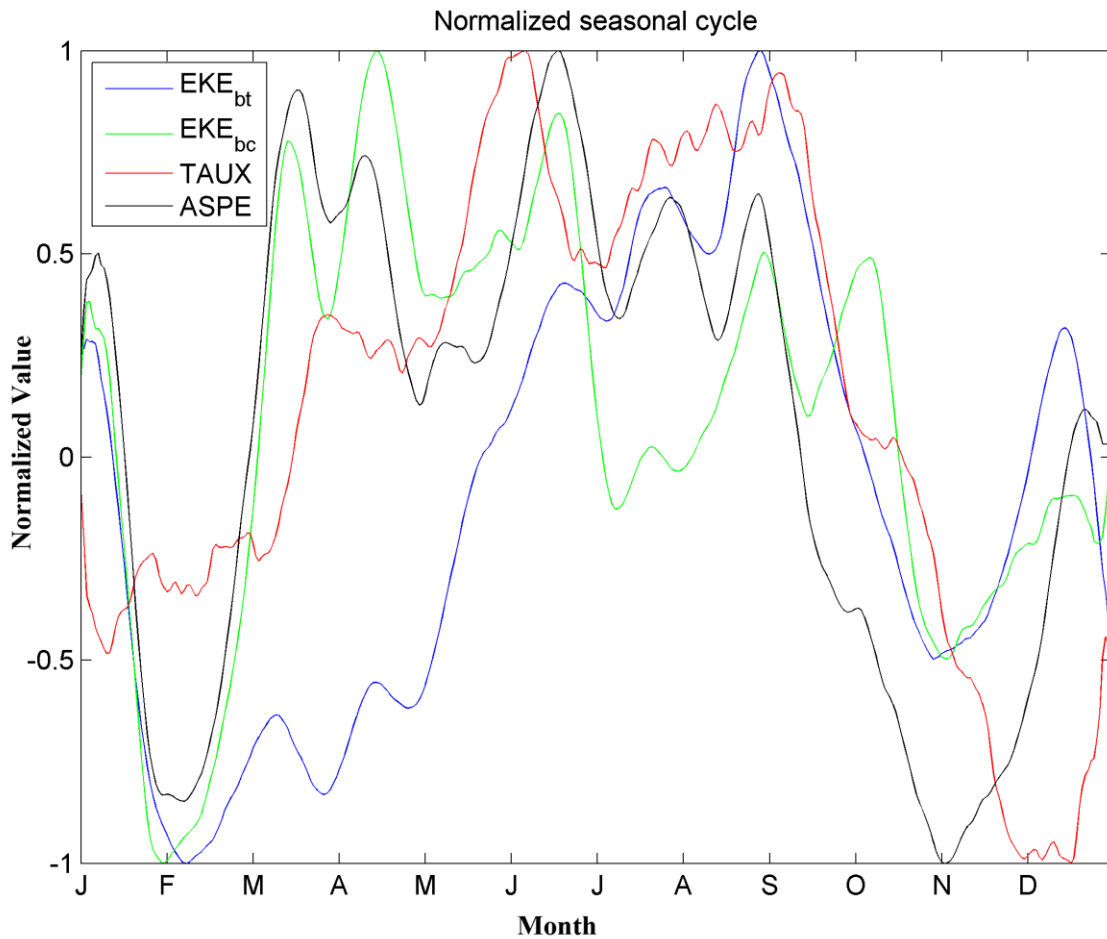


Fig. S14. Normalized seasonal cycle of ASPE, EKE_{BT} , EKE_{BC} and zonal wind stress in the scale of >50 km over the STCC region, based on the converted ROMS data. The correlation coefficients between the ASPE and two EKE components (EKE_{BT} , EKE_{BC}) are 0.40 and 0.78, separately.